HHS Public Access

Author manuscript

Cell Rep. Author manuscript; available in PMC 2018 March 07.

Published in final edited form as:

Cell Rep. 2017 November 21; 21(8): 2058–2065. doi:10.1016/j.celrep.2017.10.098.

Biological Significance of the Suppression of Oxidative Phosphorylation in Induced Pluripotent Stem Cells

Cheng Zhang[3], **Maria Skamagki**[1,2], **Zhong Liu**[4], **Aparna Ananthanarayanan**[1,2], **Rui Zhao**[4,*], **Hu Li**[3,*], and **Kitai Kim**[1,2,5,*]

[1]Cancer Biology and Genetics Program, The Center for Cell Engineering, The Center for Stem Cell Biology, Memorial Sloan Kettering Cancer Center, Sloan Kettering Institute for Cancer Research, New York, NY 10065, USA

[2]Department of Cell and Developmental Biology, Weill Medical College of Cornell University, New York, NY 10065, USA

[3]Department of Molecular Pharmacology & Experimental Therapeutics, Center for Individualized Medicine, Mayo Clinic College of Medicine, Rochester, MN 55902, USA

[4]Department of Biochemistry and Molecular Genetics, Gregory Fleming James Cystic Fibrosis Research Center, University of Alabama at Birmingham, Birmingham, AL 35294, USA

SUMMARY

We discovered that induced pluripotent stem cell (iPSC) clones generated from aged tissue donors (A-iPSCs) fail to suppress oxidative phosphorylation. Compared to embryonic stem cells (ESCs) and iPSCs generated from young donors (Y-iPSCs), A-iPSCs show poor expression of the pluripotent stem cell-specific glucose transporter 3 (GLUT3) and impaired glucose uptake, making them unable to support the high glucose demands of glycolysis. Persistent oxidative phosphorylation in A-iPSCs generates higher levels of reactive oxygen species (ROS), which leads to excessive elevation of glutathione (a ROS-scavenging metabolite) and a blunted DNA damage response. These phenotypes were recapitulated in Y-iPSCs by inhibiting pyruvate dehydrogenase kinase (PDK) or supplying citrate to activate oxidative phosphorylation. In addition, oxidative phosphorylation in A-iPSC clones depletes citrate, a nuclear source of acetyl group donors for histone acetylation; this consequently alters histone acetylation status. Expression of GLUT3 in A-iPSCs recovers the metabolic defect, DNA damage response, and histone acetylation status.

In Brief

*Correspondence: ruizhao@uab.edu (R.Z.), li.hu@mayo.edu (H.L.), kimk@mskcc.org (K.K.).
[5]Lead Contact

DATA AND SOFTWARE AVAILABILITY

The accession number for the data reported in this paper is GEO: GSE85365.

SUPPLEMENTAL INFORMATION

Supplemental Information includes Supplemental Experimental Procedures and four figures and can be found with this article online at https://doi.org/10.1016/j.celrep.2017.10.098.

AUTHOR CONTRIBUTIONS

M.S., R.Z., H.L., and K.K. conceived the experimental plan. C.Z., M.S., Z.L., A.A., R.Z., and K.K. performed the experiments. C.Z. and H.L. performed computational analysis. C.Z., M.S., R.Z., H.L., and K.K. wrote the manuscript.

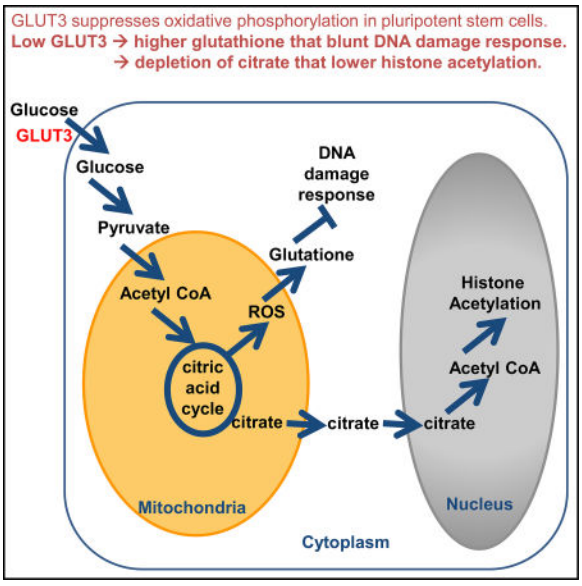

Zhang et al. demonstrate that GLUT3 suppresses somatic cell-specific oxidative phosphorylation in pluripotent stem cells. Low GLUT3 results in higher glutathione, blunting the DNA damage response, and citrate depletion, reducing histone acetylation. Expression of GLUT3 restores regulation.

INTRODUCTION

The homeostatic balance of the redox status in the cytoplasm (glycolysis) and in mitochondria (oxidative phosphorylation) governs the production of energy and building blocks in cells, broadly influencing the biological functions of every cell type in all living organisms (O'Rourke, 2016). A transition in the cytosolic and mitochondrial redox status occurs when cells change their properties, in both normal cellular transitions (e.g., tissue differentiation, embryo development, and stem cell reprogramming) and in cellular dysfunction (e.g., neurodegeneration, diabetes, cardiovascular diseases, and cancer) (Kang and Pervaiz, 2012). An understanding of the biological mechanisms and functional defects that perturb the redox status has significant implications for basic cell biology and cell-based therapies.

Pluripotent stem cells such as embryonic stem cells (ESCs) and induced pluripotent stem cells (iPSCs) favor hypoxic conditions for self-renewal and pluripotency by suppressing oxidative phosphorylation and minimizing both oxygen use and the production of reactive oxygen species (ROS) (Mathieu et al., 2014; Zhang et al., 2012; Folmes et al., 2011). Pluripotent stem cells show relatively higher oxidative phosphorylation levels when in the naive state than in the primed state (Huang et al., 2014; Zhou et al., 2012; Takashima et al., 2014). A hypoxic state also promotes the reprogramming of somatic cells to iPSCs (Yoshida et al., 2009). During iPSC reprogramming, a switch occurs in glucose metabolism, in which somatic cell-specific oxidative phosphorylation is suppressed and pluripotent stem cell-specific glycolysis is supported (Ezashi et al., 2005; Facucho-Oliveira et al., 2007). However, the biological consequence of suppressing oxidative phosphorylation during

reprogramming of pluripotent stem cells has not been studied because all pluripotent stem cells use glycolysis. In our study of the mechanism behind the redox changes, we used mouse iPSC and ESC models with a fixed congenic genetic background (B6CBA), which allowed us to directly compare various cell types with minimum genetic variability. We discovered that iPSC clones generated from aged tissue donors (A-iPSCs, 1.4-year-old tail-tip fibroblasts) fail to suppress oxidative phosphorylation, while iPSCs generated from young tissue donors (Y-iPSCs, 5-day-old neonate tail-tip fibroblasts) and ESCs switched from oxidative phosphorylation to glycolysis. Thus, A-iPSCs provided us with a unique tool to study the biological significance of suppressing oxidative phosphorylation in pluripotent stem cells.

Under the hypoxic conditions that favor pluripotent stem cell self-renewal, the suppression of oxidative phosphorylation also reduces ROS generation. Excessive ROS levels and aberrant activation of downstream pathways in somatic cells have been shown to block self-renewal and iPSC reprogramming (Hong et al., 2009; Li et al., 2009; Utikal et al., 2009). A key regulator of cellular ROS level is glutathione (a ROS-scavenging metabolite); the balance between ROS and glutathione is important to minimize oxidative damage and trigger the DNA damage response leading to apoptosis. Chemotherapy-resistant cancers show an imbalance in ROS-glutathione and a defect in apoptosis (Traverso et al., 2013; Balendiran et al., 2004). We observed a similar imbalance in ROS-glutathione homeostasis in A-iPSCs, in which high levels of ROS led to excessive glutathione and a subsequent blunting of the DNA damage response (Skamagki et al., 2017).

Using A-iPSCs as a tool, we investigated the mechanisms and downstream consequences of persistent oxidative phosphorylation compared to Y-iPSCs and ESCs. We found that suppression of oxidative phosphorylation is essential for supporting the DNA damage response in iPSC reprogramming and for maintaining histone acetylation. Our findings shed light on the biological significance of the redox status during both normal cellular transitions and cellular dysfunction.

RESULTS

A-iPSCs Have Impaired Glucose Uptake and Altered Glucose Metabolism

Because metabolic alterations are key drivers of somatic cell aging (Finkel, 2015) and changes in metabolism have been noted during the reprogramming of somatic cells to iPSCs (Shyh-Chang et al., 2013a), we compared the metabolic differences in A-iPSCs and Y-iPSCs. Others have reported that somatic cells favor oxidative phosphorylation to generate ATP, while pluripotent stem cells primarily use glycolysis (Shyh-Chang et al., 2013a; Zhang et al., 2012). In our previous report (Skamagki et al., 2017), we generated Y-iPSCs (from skin fibroblasts from 5-day-old neonatal mice) and A-iPSCs (from skin fibroblasts from 1.4-year-old mice) using the standard Yamanaka iPSC reprogramming methods (Skamagki et al., 2017), as described previously (Kim et al., 2010, 2011; Lister et al., 2009; Ohi et al., 2011). We confirmed the pluripotency of Y-iPSCs and A-iPSCs by AP1/SSEA1/OCT4/NANOG expression, teratoma analysis, and chimera analysis (Skamagki et al., 2017; Kim et al., 2010; Smith et al., 2009) (Figures S1A–S1D).

We performed a comparative gene expression analysis, and we found that A-iPSCs poorly expressed pluripotent stem cell-specific glucose transporter 3 (GLUT3) compared to Y-iPSCs (Figures 1A and 1B). GLUT3 has a high affinity for glucose (Maher et al., 1996), and glucose uptake in A-iPSCs was impaired relative to Y-iPSCs (Figure 1C). Glycolysis was inefficient and only generated 2 ATP from 1 glucose. By contrast, oxidative phosphorylation efficiently generated 36 ATP from 1 glucose. Thus, we hypothesized that A-iPSCs are unable to support active glycolysis due to the decrease in GLUT3 and poor glucose uptake. XF^e96 extracellular flux analysis (Ho et al., 2012) confirmed that A-iPSCs underwent more oxidative phosphorylation, with greater O_2 consumption, compared to Y-iPSCs and ESCs (Figure 1D; Figures S1E–S1H) (Ferrick et al., 2008). Together, our results suggest that A-iPSCs cannot take in sufficient glucose to support glycolitic capacity (Figures S1I–S1L), and thus they continue to use somatic cell-specific oxidative phosphorylation.

Persistent Oxidative Phosphorylation in A-iPSCs Leads to an Imbalance in ROS-Glutathione Homeostasis that Blunts the DNA Damage Response

We conducted global liquid chromatography-mass spectrometry (LC-MS) metabolite analysis as a pilot experiment in A-iPSCs, ESCs, and Y-iPSCs to measure 161 metabolites. Metabolite analysis confirmed the metabolic alterations in A-iPSCs (Figures S2A–S2E) (da Silva et al., 2013). Ontogenic analysis of the detected metabolites defined differential metabolic signatures, with the topmost pathway related to glutathione synthesis (Figure S2C).

Persistent oxidative phosphorylation in A-iPSCs (Figure S1G) may fuel chronic ROS production (Ray et al., 2012) and trigger an increase in glutathione, a ROS-scavenging metabolite (Shyh-Chang et al., 2013a; Zhang et al., 2012), to counteract the increase in ROS. We detected a number of differentially regulated metabolites in the glutathione pathway in A-iPSCs compared to Y-iPSCs and ESCs, including a chronic elevation of glutathione (Figure 2A). This indicated active glutathione synthesis in response to either excessive production or extensive consumption of the intermediate metabolites in A-iPSCs. Excessive glutathione activity in A-iPSCs (Figure 2A) corresponded to excessive scavenging of ROS (Figure 2B) (Johnson et al., 2012), and it was confirmed by the induction of ROS upon treatment of A-iPSCs with the glutathione synthetase (GSS) pharmacological inhibitor L-Buthionine-sulfoximine (BSO) (Figure S2F).

ROS not only damages DNA but also plays a protective role by inducing the DNA damage response to environmental stressors. Excessive glutathione activity and depletion of ROS may impair the DNA damage response in A-iPSCs (Skamagki et al., 2017); this effect of excessive glutathione activity has been reported in chemotherapy-resistant cancers (Traverso et al., 2013; Balendiran et al., 2004). Treatment of A-iPSCs with phleomycin (a structural analog of bleomycin with higher potency) to induce DNA double-strand breaks revealed a blunted DNA damage response (ataxia telangiectasia mutated [ATM] pathway) compared to Y-iPSCs and ESCs (Figure 2C; Skamagki et al., 2017).

Recovering GLUT3 Expression in A-iPSCs Restores Stem-Cell-Specific Glucose Metabolism and the DNA Damage Response

The pluripotent-specific suppression of oxidative phosphorylation and switch to glycolysis requires a high level of glucose import to support relatively inefficient glycolysis. Therefore, we hypothesized that the failure to suppress oxidative phosphorylation by A-iPSCs is a consequence of insufficient glucose uptake caused by a defect in GLUT3 expression. We found that expression of GLUT3 during A-iPSC reprogramming (Figures S1A–S1D) recovered GLUT3 expression (Figure 1B) and glucose uptake (Figure 1C), and it led to the suppression of oxidative phosphorylation (Figure 1D). Suppression of oxidative phosphorylation upon GLUT3 expression in A-iPSCs normalized the glutathione metabolic pathway (Figure 2A), restored the balance between ROS and glutathione (Figures 2A and 2B), and recovered the DNA damage response (Figure 2C) and apoptosis in response to stress (Figures 2D and 2E) to levels comparable to those of ESCs and Y-iPSCs. Ablation of GLUT3 in Y-iPSCs recapitulated the phenotype of A-iPSCs, leading to a loss of the DNA damage response (Figures S2G and S2H) and apoptosis in response to stress (Figures 2D and 2E), a decrease in glucose uptake (Figure 2F) and ROS (Figure 2G), and an increase in O_2 consumption rate (OCR) (Figure 2H) and glutathione (Figure 2I).

Recapitulation of the Consequences of Persistent Oxidative Phosphorylation in Y-iPSCs by Pyruvate Dehydrogenase Kinase Inhibition and Citrate Supplementation

Because higher pyruvate dehydrogenase kinase (PDK) activity in pluripotent stem cells blocks glucose as the carbon source for the citric acid cycle and inhibits oxidative phosphorylation (Rodrigues et al., 2015), we hypothesized that the inhibition of PDK in Y-iPSCs would activate oxidative phosphorylation and recapitulate the phenotype of A-iPSCs. A recent report showed that the PDK inhibitor dichloroacetate (DCA), a pharmacologic anticancer agent, efficiently activates oxidative phosphorylation in ESCs (Rodrigues et al., 2015). We cultured Y-iPSCs in the presence of DCA, and we found that Y-iPSCs recapitulated the A-iPSC phenotype, with activation of oxidative phosphorylation in the presence of glucose (Figure 3A). DCA-induced oxidative phosphorylation also increased ROS (Figure 3B) and apoptosis (Figure 3C). We hypothesized that Y-iPSC clones surviving after DCA treatment contain elevated glutathione to scavenge excess ROS and show an impaired DNA damage response in response to stress. Indeed, DCA treatment selected for Y-iPSC clones with high glutathione (Figure 3D) and a poor DNA damage response (Figure 3E).

We also added citrate (substrate for the citric acid cycle) to Y-iPSC culture media to confirm the downstream consequences of the persistent oxidative phosphorylation seen in A-iPSCs. Exposure of Y-iPSCs to citrate activated oxidative phosphorylation (Figure 3A) and increased ROS (Figure 3B) and apoptosis (Figure 3C). The surviving Y-iPSC clones contained elevated glutathione (Figure 3D), showed a poor DNA damage response to stress (Figure 3E), and had excessive scavenging of ROS (Figure 3F).

Persistent Oxidative Phosphorylation in A-iPSCs Depletes Citrate and Alters the Pluripotent Histone Acetylation Status

Citrate is the key metabolite in the citric acid cycle of oxidative phosphorylation (Figure S2I). A pilot global metabolite analysis showed a lower citrate level in A-iPSCs than in ESCs and Y-iPSCs (Figures S2A–S2E), indicating that either production of citrate is lower or it is catabolized faster in A-iPSCs. This result was confirmed by targeted citrate metabolite analysis (Figure 4A). Because the oxygen production rate in A-iPSCs is greater than in ESCs and Y-iPSCs (Figure 1D), the lower citrate level in A-iPSCs is likely due to depletion through a highly active citric acid cycle with limited carbon sources.

Mitochondrial acetyl-CoA enters the citric acid cycle to produce citrate, which can be transported across the mitochondrial membrane and used to produce acetyl-CoA in the nucleus and cytoplasm. Citrate is a source of acetyl-CoA, which is a substrate for histone acetylation in the nucleus (Figure S2I) (Choudhary et al., 2014). In ESCs and Y-iPSCs, acetyl-CoA produced from threonine proteolysis or alternative carbon sources (Shyh-Chang et al., 2013b) is sufficient to maintain citrate metabolite concentrations to support the production of acetyl-CoA in the nucleus. Because A-iPSCs generate citrate from limited alternative carbon sources and consume citrate in the citric acid cycle as part of oxidative phosphorylation, less citrate is available for producing acetyl-CoA in the nucleus. We therefore hypothesized that histone acetylation levels in A-iPSCs would be lower than in ESCs/Y-iPSCs as a consequence of the differences in citrate concentration.

We quantified 99 histone modifications in A-iPSCs, ESCs, and Y-iPSCs using histone post-translational modification profiling with MS analysis (Yuan et al., 2015; Feller et al., 2015). We found statistically significant histone modifications (Figure 4B) with major changes in histone acetylation. Exogenous expression of GLUT3 in A-iPSCs to suppress oxidative phosphorylation (Figure 1D) recovered citrate to the levels seen in ESCs and Y-iPSCs (Figure 4A). GLUT3 expression also increased histone acetylation (Figure 4B) in A-iPSCs to levels equivalent to those in ESCs and Y-iPSCs.

ZSCAN10 as an Upstream Transcriptional Regulator of GLUT3 Expression

In an independent series of studies, we found that a newly identified pluripotent stem cell-specific transcription factor, ZSCAN10, is deficient in A-iPSCs (Skamagki et al., 2017). When expressed in A-iPSCs, ZSCAN10 normalized GLUT3 expression (Figure S3A), glucose uptake (Figure S3B), oxidative phosphorylation rate (Figure S3C), and homeostatic balance between ROS and glutathione (Figures S3D and S3E), similar to what was seen with exogenous GLUT3 expression. A previous report (Yu et al., 2009) showed by chromatin immunoprecipitation (ChIP)-on-ChIP analysis that ZSCAN10 directly binds to the *Gluts3* promoter; we confirmed this interaction by ChIP-qPCR (Figure S3F).

DISCUSSION

In this study, we found that A-iPSCs show persistent oxidative phosphorylation whereas Y-iPSCs and ESCs rely predominantly on glycolysis. Thus, A-iPSCs presented us with a unique research tool to study the consequences of a failure to suppress oxidative

phosphorylation during reprogramming. We also found that A-iPSCs express lower levels of GLUT3 and its regulator, ZSCAN10 (Skamagki et al., 2017), and that suppression of oxidative phosphorylation could be achieved with exogenous GLUT3 expression. Conversely, we recapitulated the negative effects of persistent oxidative phosphorylation (ROS elevation, ROS-glutathione imbalance, poor DNA damage response, and altered histone acetylation) in Y-iPSCs treated with a PDK inhibitor or citrate. These experiments reveal the biological significance of the redox status during stem cell reprogramming, and they have implications for the role of redox status in other cellular transitions, such as tissue differentiation, embryo development, cellular degeneration, and cancer development (Kang and Pervaiz, 2012).

Previous studies have shown that the metabolic switch from oxidative phosphorylation to glycolysis involves the activation of PDK, which inhibits pyruvate dehydrogenase and the conversion of pyruvate to acetyl-CoA that fuels oxidative phosphorylation (Zhang et al., 2012; Shyh-Chang et al., 2013a). We hypothesized that, in addition to expressing lower levels of GLUT3 and taking up less glucose, A-iPSCs fail to activate PDK, allowing continued pyruvate decarboxylation and the production of acetyl-CoA for oxidative phosphorylation. However, ESCs, Y-iPSCs, and A-iPSCs all showed higher levels of PDK and PDK activity compared with fibroblasts (Figures S4A–S4C), but differential GLUT3 expression patterns (Figure S4B), suggesting that A-iPSCs must suppress pyruvate decarboxylation to block the glucose carbon source that fuels the oxidative phosphorylation seen in ESCs and Y-iPSCs. Therefore, we examined whether A-iPSCs use an alternative carbon source (Shyh-Chang et al., 2013a). Amino acids are used as an alternative carbon source in a number of cancer cells and somatic cells (Shyh-Chang et al., 2013a). YSI biochemistry analysis showed that the most abundant amino acid in serum, glutamine (Zhang et al., 2012; Shyh-Chang et al., 2013a), is more actively consumed in A-iPSCs compared to ESCs and Y-iPSCs (Figure S4D) (Mitra et al., 2015). This result indicated that A-iPSCs use more glutamine or other alternative carbon sources, such as other amino acids and lipids, to sustain oxidative phosphorylation (Figure 1D). We also tested whether lipids are an alternative carbon source in A-iPSCs, but we did not observe a significant difference between the cell types (Figure S4E). The full list of alternative carbon sources used by A-iPSCs remains to be determined.

Our previous report demonstrated that epigenetic memory from the somatic cell of origin influences the features of the resulting iPSCs (Kim et al., 2010). Here we show that metabolic differences in somatic cells could affect the epigenome and biological features of the resulting iPSCs. However, we did not see significant metabolic differences between the somatic cells from young and aged donors (Figures S4F and S4G). It is difficult to determine whether differences in GLUT3 expression and activity in Y-iPSCs and A-iPSCs are due to the epigenetic memory of young and aged donor cells, because GLUT3 is not expressed in somatic cells. Nevertheless, there may be an indirect mechanism regulating GLUT3 expression in iPSCs via age-related epigenetic differences in somatic cells that regulate expression of the upstream regulator ZSCAN10.

Expression of GLUT3 during A-iPSC reprogramming increases glucose uptake, which would provide cells with sufficient energy to drive glycolysis, making cells less dependent

on oxidative phosphorylation. As a result, more citrate will be present in mitochondria due to reduced consumption by less active oxidative phosphorylation. Excess mitochondrial citrate can be exported to the cytoplasm and converted to acetyl-CoA (Moussaieff et al., 2015), which then enters the nucleus and serves as the donor for histone acetylation in pluripotent stem cells (Shyh-Chang and Daley, 2015). This question can be further analyzed with DCA and citrate treatments; however, transient DCA and citrate treatment induced Y-iPSC cell death and differentiation. After stopping treatment, the few surviving clones that had not undergone differentiation demonstrated the consequences of selective activation of oxidative phosphorylation in iPSCs. Like A-iPSCs, these cells showed a homeostatic imbalance between ROS and glutathione and a blunted DNA damage response. The effects of DCA or citrate treatment on histone acetylation were only seen with continuous treatment, which generated a mixed population of dying and partially differentiated Y-iPSCs. The lack of a stable and homogeneous sample after prolonged citrate treatment made it difficult to evaluate the impact on histone acetylation in Y-iPSCs. Nevertheless, our study revealed an effect on histone acetylation of citrate depletion by sustained oxidative phosphorylation in A-iPSCs and recovery of citrate levels and histone acetylation by GLUT3 expression. The downstream effects of aberrant glucose metabolism on histone acetylation and diverse regulatory pathways in various organisms remain to be investigated.

EXPERIMENTAL PROCEDURES

Mouse ESCs and iPSCs were cultured in ESC media containing 15% fetal bovine serum (FBS) and 1,000 U/mL leukemia inhibitory factor (LIF). For reprogramming of somatic cells, retrovirus expressing OCT4, SOX2, KLF4, and MYC was introduced. For somatic cells containing inducible reprogramming factors, the media were supplemented with 2 μg/mL doxycycline. For DNA and RNA isolation, ESCs or iPSCs were trypsinized and replated onto new tissue culture dishes for 45 min to remove feeder cells, and nucleic acids were extracted from the nonadherent cell suspension. Information regarding cell lines, antibodies, plasmids, and drugs used in this study, as well as detailed protocols for reprogramming and cell culture, overexpression and knockdown, gene expression analysis (qPCR), immunofluorescence staining and analysis, immunoblot analysis, retrovirus and lentivirus production, drug treatments and irradiation, teratoma analysis, glutathione detection assay, and ROS assay are provided in the Supplemental Experimental Procedures. All experimental processes with animal subjects were conducted under oversight by an institutional review board (IACUC Protocol #: 11-10-023).

Supplementary Material

Refer to Web version on PubMed Central for supplementary material.

Acknowledgments

K.K. is supported by the NIH (R00HL093212 and R01AG043531), TriStem-Star Foundation (2013-049), Louis V. Gerstner, Jr. Young Investigators awards, Geoffrey Beene Junior Chair Award, Sidney Kimmel Scholar Award, Alfred W. Bressler Scholars Endowment Fund, and MSKCC Society Fund. MSKCC Core Facilities are supported by NIH Cancer Center support grant P30 CA008748. H.L. is supported by NIH (CA196631-01A1), Mayo Clinic Center for Individualized Medicine, and by a grant from the Paul F. Glenn Foundation. R.Z. is supported by the UAB startup fund, UAB Faculty Development Fund, and UAB CFRC Pilot & Feasibility Grant (ROWE15R0).

Metabolic analysis including YSI analysis was supported by the Donald B. and Catherine C. Marron Cancer Metabolism Center, MSKCC (director, Dr. Justin Cross), New York, NY, USA.

References

Balendiran GK, Dabur R, Fraser D. The role of glutathione in cancer. Cell Biochem. Funct. 2004; 22:343–352. [PubMed: 15386533]

Choudhary C, Weinert BT, Nishida Y, Verdin E, Mann M. The growing landscape of lysine acetylation links metabolism and cell signalling. Nat. Rev. Mol. Cell Biol. 2014; 15:536–550. [PubMed: 25053359]

da Silva VR, Rios-Avila L, Lamers Y, Ralat MA, Midttun Ø, Quinlivan EP, Garrett TJ, Coats B, Shankar MN, Percival SS, et al. Metabolite profile analysis reveals functional effects of 28-day vitamin B-6 restriction on one-carbon metabolism and tryptophan catabolic pathways in healthy men and women. J. Nutr. 2013; 143:1719–1727. [PubMed: 23966327]

Ezashi T, Das P, Roberts RM. Low O2 tensions and the prevention of differentiation of hES cells. Proc. Natl. Acad. Sci. USA. 2005; 102:4783–4788. [PubMed: 15772165]

Facucho-Oliveira JM, Alderson J, Spikings EC, Egginton S, St John JC. Mitochondrial DNA replication during differentiation of murine embryonic stem cells. J. Cell Sci. 2007; 120:4025–4034. [PubMed: 17971411]

Feller C, Forné I, Imhof A, Becker PB. Global and specific responses of the histone acetylome to systematic perturbation. Mol. Cell. 2015; 57:559–571. [PubMed: 25578876]

Ferrick DA, Neilson A, Beeson C. Advances in measuring cellular bioenergetics using extracellular flux. Drug Discov. Today. 2008; 13:268–274. [PubMed: 18342804]

Finkel T. The metabolic regulation of aging. Nat. Med. 2015; 21:1416–1423. [PubMed: 26646498]

Folmes CD, Nelson TJ, Martinez-Fernandez A, Arrell DK, Lindor JZ, Dzeja PP, Ikeda Y, Perez-Terzic C, Terzic A. Somatic oxidative bioenergetics transitions into pluripotency-dependent glycolysis to facilitate nuclear reprogramming. Cell Metab. 2011; 14:264–271. [PubMed: 21803296]

Ho J, de Moura MB, Lin Y, Vincent G, Thorne S, Duncan LM, Hui-Min L, Kirkwood JM, Becker D, Van Houten B, Moschos SJ. Importance of glycolysis and oxidative phosphorylation in advanced melanoma. Mol. Cancer. 2012; 11:76. [PubMed: 23043612]

Hong H, Takahashi K, Ichisaka T, Aoi T, Kanagawa O, Nakagawa M, Okita K, Yamanaka S. Suppression of induced pluripotent stem cell generation by the p53-p21 pathway. Nature. 2009; 460:1132–1135. [PubMed: 19668191]

Huang K, Maruyama T, Fan G. The naive state of human pluripotent stem cells: a synthesis of stem cell and preimplantation embryo transcriptome analyses. Cell Stem Cell. 2014; 15:410–415. [PubMed: 25280217]

Johnson WM, Wilson-Delfosse AL, Mieyal JJ. Dysregulation of glutathione homeostasis in neurodegenerative diseases. Nutrients. 2012; 4:1399–1440. [PubMed: 23201762]

Kang J, Pervaiz S. Mitochondria: redox metabolism and dysfunction. Biochem. Res. Int. 2012; 2012:896751. [PubMed: 22593827]

Karner CM, Esen E, Chen J, Hsu FF, Turk J, Long F. Wnt Protein Signaling Reduces Nuclear Acetyl-CoA Levels to Suppress Gene Expression during Osteoblast Differentiation. J. Biol. Chem. 2016; 291:13028–13039. [PubMed: 27129247]

Kim K, Doi A, Wen B, Ng K, Zhao R, Cahan P, Kim J, Aryee MJ, Ji H, Ehrlich LI, et al. Epigenetic memory in induced pluripotent stem cells. Nature. 2010; 467:285–290. [PubMed: 20644535]

Kim K, Zhao R, Doi A, Ng K, Unternaehrer J, Cahan P, Huo H, Loh YH, Aryee MJ, Lensch MW, et al. Donor cell type can influence the epigenome and differentiation potential of human induced pluripotent stem cells. Nat. Biotechnol. 2011; 29:1117–1119. [PubMed: 22119740]

Li H, Collado M, Villasante A, Strati K, Ortega S, Cañamero M, Blasco MA, Serrano M. The Ink4/Arf locus is a barrier for iPS cell reprogramming. Nature. 2009; 460:1136–1139. [PubMed: 19668188]

Lister R, Pelizzola M, Dowen RH, Hawkins RD, Hon G, Tonti-Filippini J, Nery JR, Lee L, Ye Z, Ngo QM, et al. Human DNA methylomes at base resolution show widespread epigenomic differences. Nature. 2009; 462:315–322. [PubMed: 19829295]

Maher F, Davies-Hill TM, Simpson IA. Substrate specificity and kinetic parameters of GLUT3 in rat cerebellar granule neurons. Biochem. J. 1996; 315:827–831. [PubMed: 8645164]

Mathieu J, Zhou W, Xing Y, Sperber H, Ferreccio A, Agoston Z, Kuppusamy KT, Moon RT, Ruohola-Baker H. Hypoxia-inducible factors have distinct and stage-specific roles during reprogramming of human cells to pluripotency. Cell Stem Cell. 2014; 14:592–605. [PubMed: 24656769]

Mitra S, Molina J, Mills GB, Dennison JB. Characterization of the role Rab25 in energy metabolism and cancer using extracellular flux analysis and material balance. Methods Mol. Biol. 2015; 1298:195–205. [PubMed: 25800844]

Moussaieff A, Rouleau M, Kitsberg D, Cohen M, Levy G, Barasch D, Nemirovski A, Shen-Orr S, Laevsky I, Amit M, et al. Glycolysis-mediated changes in acetyl-CoA and histone acetylation control the early differentiation of embryonic stem cells. Cell Metab. 2015; 21:392–402. [PubMed: 25738455]

O'Rourke B. Metabolism: Beyond the power of mitochondria. Nat. Rev. Cardiol. 2016; 13:386–388. [PubMed: 27303815]

Ohi Y, Qin H, Hong C, Blouin L, Polo JM, Guo T, Qi Z, Downey SL, Manos PD, Rossi DJ, et al. Incomplete DNA methylation underlies a transcriptional memory of somatic cells in human iPS cells. Nat. Cell Biol. 2011; 13:541–549. [PubMed: 21499256]

Ray PD, Huang BW, Tsuji Y. Reactive oxygen species (ROS) homeostasis and redox regulation in cellular signaling. Cell. Signal. 2012; 24:981–990. [PubMed: 22286106]

Rodrigues AS, Correia M, Gomes A, Pereira SL, Perestrelo T, Sousa MI, Ramalho-Santos J. Dichloroacetate, the Pyruvate Dehydrogenase Complex and the Modulation of mESC Pluripotency. PLoS ONE. 2015; 10:e0131663. [PubMed: 26147621]

Shyh-Chang N, Daley GQ. Metabolic switches linked to pluripotency and embryonic stem cell differentiation. Cell Metab. 2015; 21:349–350. [PubMed: 25738450]

Shyh-Chang N, Daley GQ, Cantley LC. Stem cell metabolism in tissue development and aging. Development. 2013a; 140:2535–2547. [PubMed: 23715547]

Shyh-Chang N, Locasale JW, Lyssiotis CA, Zheng Y, Teo RY, Ratanasirintrawoot S, Zhang J, Onder T, Unternaehrer JJ, Zhu H, et al. Influence of threonine metabolism on S-adenosylmethionine and histone methylation. Science. 2013b; 339:222–226. [PubMed: 23118012]

Skamagki M, Correia C, Yeung P, Baslan T, Beck S, Zhang C, Ross CA, Dang L, Liu Z, Giunta S, et al. ZSCAN10 expression corrects the genomic instability of iPSCs from aged donors. Nat. Cell Biol. 2017; 19:1037–1048. [PubMed: 28846095]

Smith KP, Luong MX, Stein GS. Pluripotency: toward a gold standard for human ES and iPS cells. J. Cell. Physiol. 2009; 220:21–29. [PubMed: 19326392]

Takashima Y, Guo G, Loos R, Nichols J, Ficz G, Krueger F, Oxley D, Santos F, Clarke J, Mansfield W, et al. Resetting transcription factor control circuitry toward ground-state pluripotency in human. Cell. 2014; 158:1254–1269. [PubMed: 25215486]

Traverso N, Ricciarelli R, Nitti M, Marengo B, Furfaro AL, Pronzato MA, Marinari UM, Domenicotti C. Role of glutathione in cancer progression and chemoresistance. Oxid. Med. Cell. Longev. 2013; 2013:972913. [PubMed: 23766865]

Utikal J, Polo JM, Stadtfeld M, Maherali N, Kulalert W, Walsh RM, Khalil A, Rheinwald JG, Hochedlinger K. Immortalization eliminates a roadblock during cellular reprogramming into iPS cells. Nature. 2009; 460:1145–1148. [PubMed: 19668190]

Yoshida Y, Takahashi K, Okita K, Ichisaka T, Yamanaka S. Hypoxia enhances the generation of induced pluripotent stem cells. Cell Stem Cell. 2009; 5:237–241. [PubMed: 19716359]

Yu HB, Kunarso G, Hong FH, Stanton LW. Zfp206, Oct4, and Sox2 are integrated components of a transcriptional regulatory network in embryonic stem cells. J. Biol. Chem. 2009; 284:31327–31335. [PubMed: 19740739]

Yuan ZF, Lin S, Molden RC, Cao XJ, Bhanu NV, Wang X, Sidoli S, Liu S, Garcia BA. EpiProfile Quantifies Histone Peptides With Modifications by Extracting Retention Time and Intensity in High-resolution Mass Spectra. Mol. Cell. Proteomics. 2015; 14:1696–1707. [PubMed: 25805797]

Zhang J, Nuebel E, Daley GQ, Koehler CM, Teitell MA. Metabolic regulation in pluripotent stem cells during reprogramming and self-renewal. Cell Stem Cell. 2012; 11:589–595. [PubMed: 23122286]

Zhou W, Choi M, Margineantu D, Margaretha L, Hesson J, Cavanaugh C, Blau CA, Horwitz MS, Hockenbery D, Ware C, Ruohola-Baker H. HIF1α induced switch from bivalent to exclusively glycolytic metabolism during ESC-to-EpiSC/hESC transition. EMBO J. 2012; 31:2103–2116. [PubMed: 22446391]

Highlights

- Low GLUT3 expression in iPSCs causes poor glucose import and glycolysis support
- These iPSCs use somatic cell-specific oxidative phosphorylation (Oxphos)
- Higher Oxphos blunts DNA damage response through an imbalance of ROS and glutathione
- Higher Oxphos depletes citrate and affects the histone acetylation

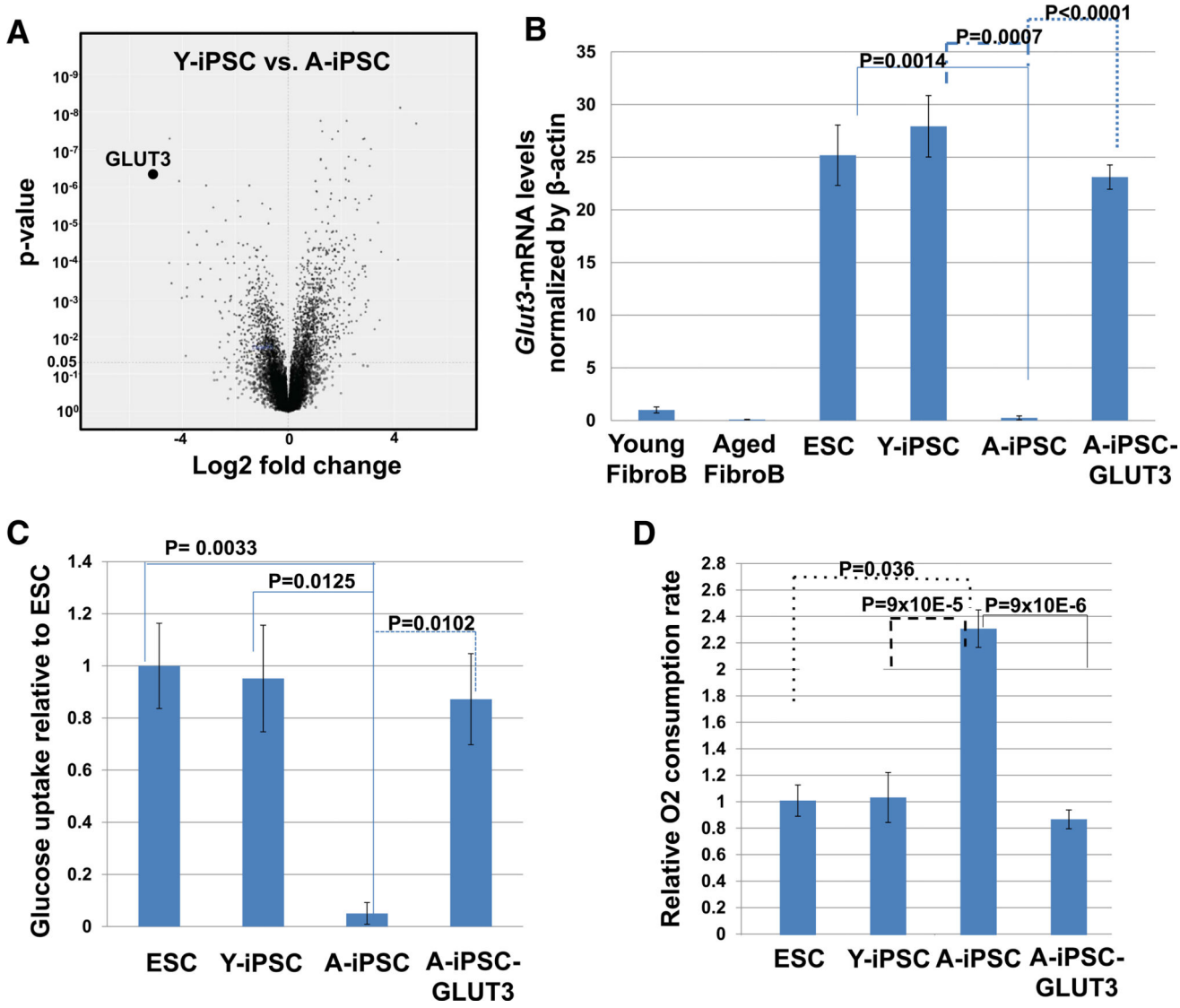

Figure 1. Altered Glucose Metabolism in A-iPSC and Recovery by GLUT3 Expression

(A) Altered GLUT3 expression from gene expression analysis. GLUT3 expression is differentially expressed in A-iPSC and Y-iPSC. At least two clonal biological repeats ($n \geq 2$) were included in the analysis.

(B) Reduced *Glut3*-mRNA levels in A-iPSC. Real-time qPCR shows that GLUT3 is not expressed in somatic cells (fibroblasts from young and aged donor mice) but is highly expressed in ESC/Y-iPSC. Endogenous GLUT3 expression is lower in A-iPSCs and upregulated by transient exogenous expression of GLUT3. Error bars indicate SEM of three independent clones in each sample group. Statistical significance was determined by two-sided t test.

(C) Glucose uptake in A-iPSC is reduced compared to ESC and Y-iPSC. GLUT3 expression in A-iPSC recovers glucose uptake rates to levels similar to ESC/Y-iPSC. Glucose uptake rate was measured with a glucose uptake analysis kit (cat#K606-100, Biovision, Milpitas,

CA, USA). Error bars indicate SEM of three independent clones in each sample group. Statistical significance was determined by two-sided t test.

(D) High level of abnormal somatic cell-specific oxidative phosphorylation in A-iPSC and recovery by GLUT3 expression. Oxidative phosphorylation rate was analyzed by measuring O_2 consumption rate (OCR) using an XF^e96 extracellular flux analyzer (Seahorse Bioscience, North Billerica, MA, USA). Error bars indicate SEM of four independent clones in each sample group. Statistical significance was determined by two-sided t test.

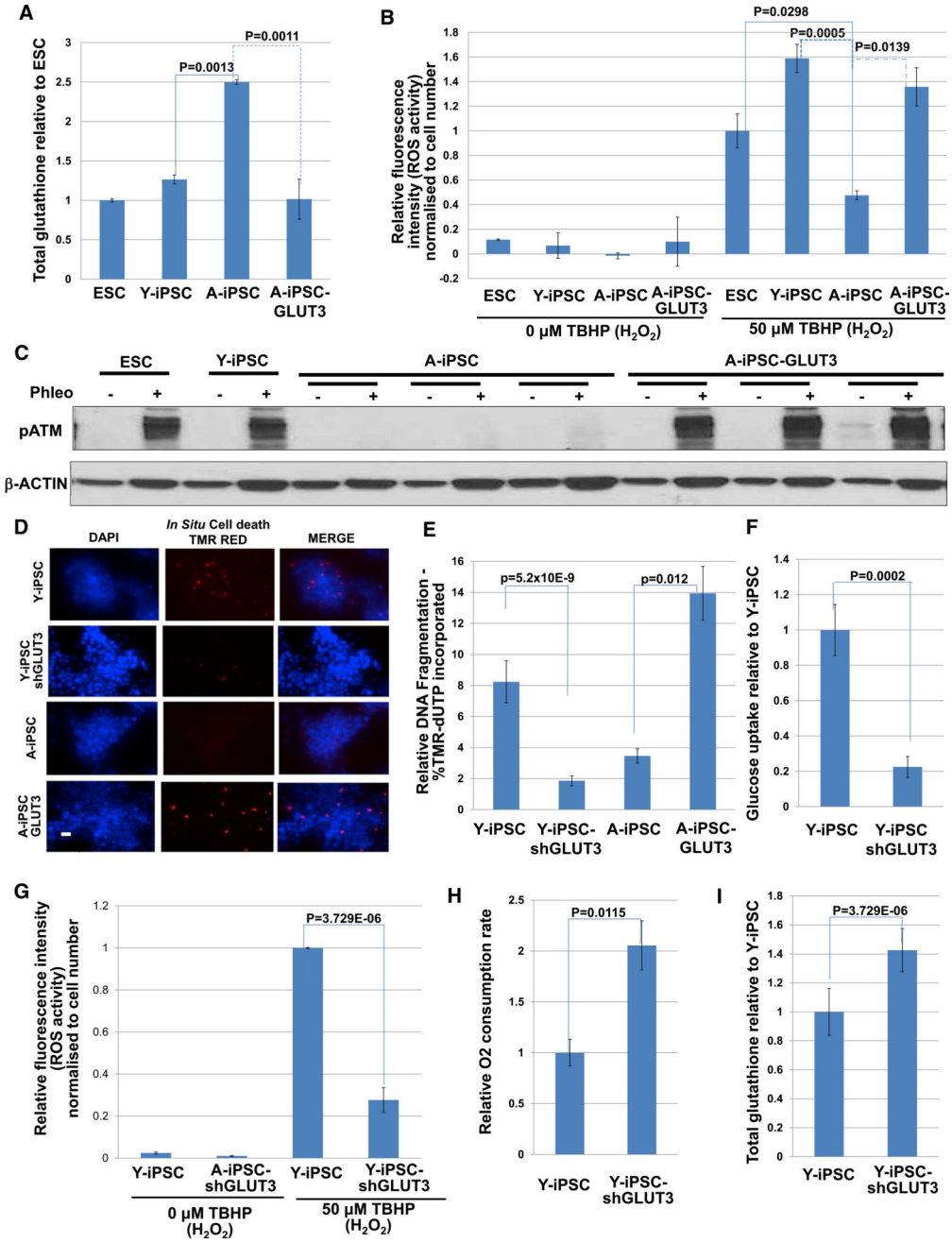

Figure 2. Imbalance in ROS-Glutathione Homeostasis that Blunts the DNA Damage Response by Persistent Oxidative Phosphorylation in A-iPSC and Recovery by GLUT3 Expression

(A) Excessive oxidation capacity with elevated glutathione in A-iPSC and recovery by GLUT3. Glutathione analysis was conducted with the glutathione fluorometric assay. Error bars indicate SEM of three biological replicates with two independent clones in each sample group. Statistical significance was determined by two-sided t test.

(B) A cellular reactive oxygen species assay kit (Abcam, ab113851) was used to measure the H_2O_2-scavenging activity of ESC, Y-iPSC, A-iPSC, and A-iPSC-GLUT3. Error bars indicate SEM of three biological replicates with two independent clones in each sample group. Statistical significance was determined by two-sided t test.

(C) Recovery of ATM phosphorylation in A-iPSC-GLUT3 compared to A-iPSC after phleomycin treatment (2 hr, 30 μg/mL), as monitored by immunoblot in three independent representative clones.

(D) *In situ* cell death assays of Y-iPSC, A-iPSC, Y-iPSC-shGLUT3, and A-iPSC-GLUT3 were performed 15 hr after the end of phleomycin treatment (2 hr, 30 μg/mL). Y-iPSC-shGLUT3 shows fewer cells staining for cell death compared to Y-iPSC and A-iPSC-GLUT3. The negative control is Y-iPSC treated with dye in the absence of enzymatic reaction. Nuclei are stained with DAPI. Scale bar indicates 100 μm.

(E) Quantification by image analysis of apoptotic response by DNA fragmentation assay after phleomycin treatment. Error bars indicate SEM of six biological replicates with three independent clones in each sample group. Statistical significance was determined by unpaired two-sided t test.

(F) Glucose uptake in Y-iPSC-shGLUT3 is reduced compared to Y-iPSC. Error bars indicate SEM of three biological replications in each sample group and two additional clones of Y-iPSC-shGLUT3. Statistical significance was determined by two-sided t test.

(G) The H_2O_2-scavenging activity of Y-iPSC and Y-iPSC-shGLUT3. Error bars indicate SEM of five biological replicates in each sample group and three additional independent clones of Y-iPSC-shGLUT3. Statistical significance was determined by two-sided t test.

(H) Excessive oxidation capacity with elevated glutathione in Y-iPSC-shGLUT3 compared with Y-iPSC. The total glutathione level was measured to determine the maximum oxidation capacity. Glutathione analysis was conducted with the glutathione fluorometric assay. Error bars indicate SEM of five biological replicates in each sample group and two additional clones of YiPSC-shGLUT3. Statistical significance was determined by two-sided t test.

(I) Excessive oxidation capacity with elevated glutathione in Y-iPSC-shGLUT3. Glutathione analysis was conducted with the glutathione fluorometric assay. Error bars indicate SEM of three biological replicates with two independent clones in each sample group. Statistical significance was determined by two-sided t test.

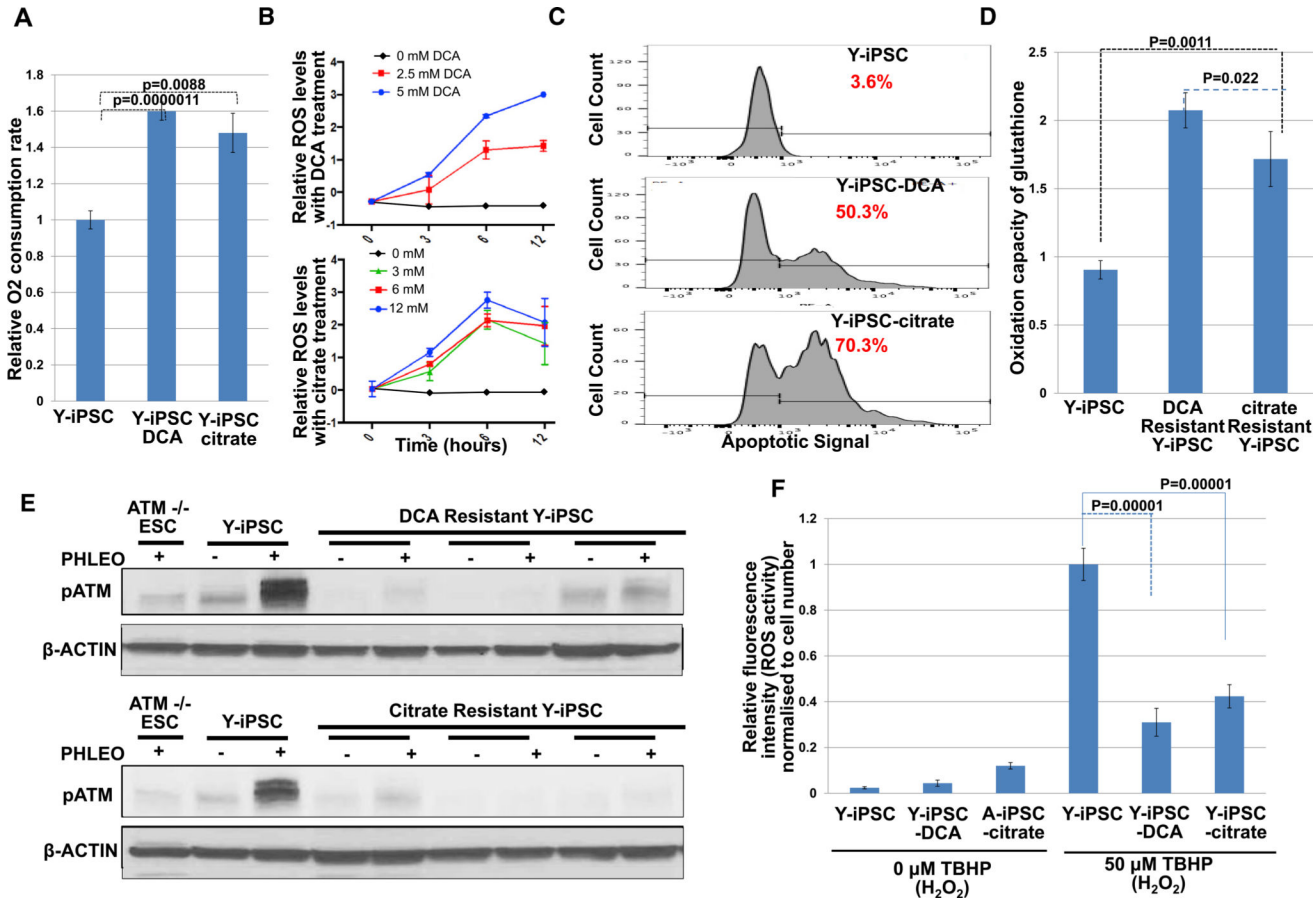

Figure 3. Recapitulation of the Consequences of Persistent Oxidative Phosphorylation in Y-iPSC by PDK Inhibition and Citrate Supplementation

(A) Excessive oxidation capacity with elevated glutathione in DCA- or sodium citrate-resistant Y-iPSC compared with Y-iPSC before DCA treatment. The total glutathione level was measured to determine the maximum oxidation capacity. Glutathione analysis was conducted with the glutathione fluorometric assay. Error bars indicate SEM of four clonal biological replicates in each sample group. Statistical significance was determined by two-sided t test.

(B) Measurement of ROS level in Y-iPSC with superoxide indicator dye (mitoSOX, Thermo Fisher Scientific, M36008) after supplementing with different concentrations of DCA or sodium citrate.

(C) Quantification of *in situ* cell death with DCA (5 mM) and citrate (3 mM) treatments in Y-iPSC by flow cytometry analysis. DNA fragmentation assays were performed 12 hr after the end of DCA and sodium citrate treatments using an *in situ* cell death assay kit (Roche) for visualization of DNA strand breaks.

(D) Excessive oxidation capacity with elevated glutathione in DCA- or sodium citrate-resistant Y-iPSC compared with Y-iPSC before DCA treatment. Total glutathione level was measured to determine the maximum oxidation capacity. Glutathione analysis was conducted with the glutathione fluorometric assay. Error bars indicate SEM of three clonal biological replicates in each sample group. Statistical significance was determined by two-sided t test.

(E) Reduced ATM phosphorylation (pATM) in DCA- or sodium citrate-resistant Y-iPSC, as monitored by immunoblot after phleomycin treatment (2 hr, 30 μg/mL) in three independent clones.

(F) A cellular reactive oxygen species assay kit was used to measure the H_2O_2-scavenging activity of Y-iPSC, Y-iPSC-DCA, and Y-iPSC-citrate. Error bars indicate SEM of five biological replicates with a parental Y-iPSC clone and three independent clones in each sample group treated with DCA and citrate. Statistical significance was determined by two-sided t test.

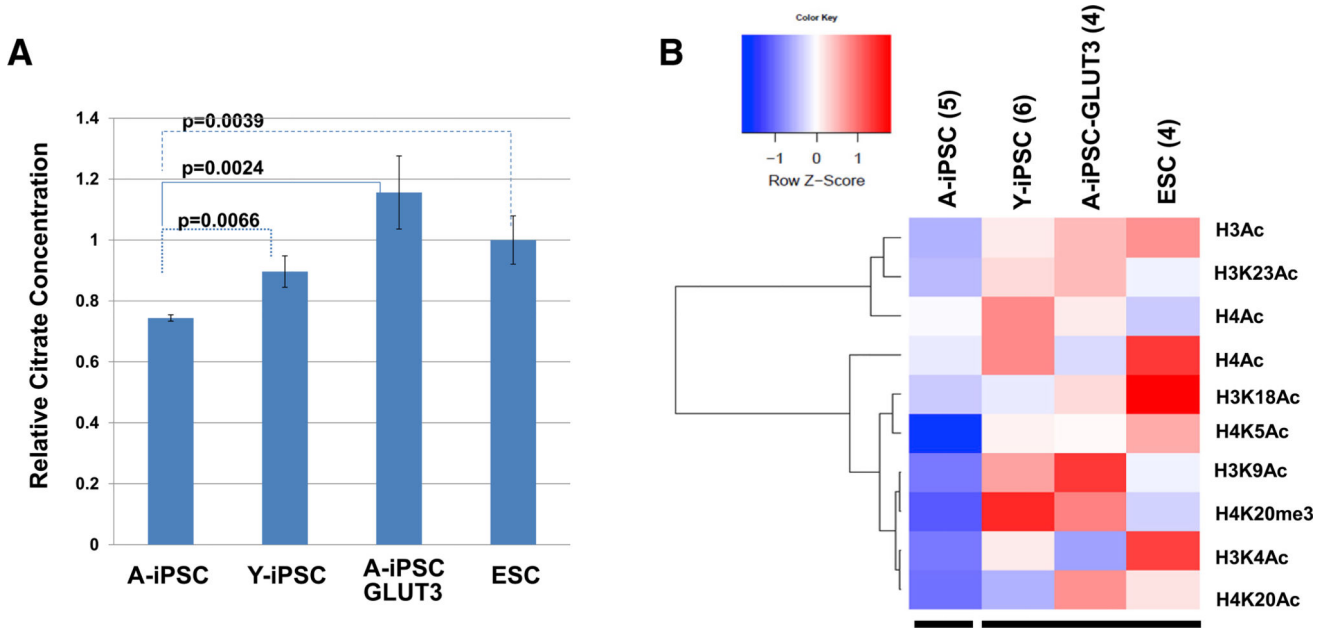

Figure 4. Depletion of Citrate as a Nuclear Acetyl Donor for Histone Modification in A-iPSC and Recovery by GLUT3 Expression

(A) Fluorometric citrate quantification analysis (Sigma, MAK057) (Karner et al., 2016) of ESC, A-iPSC, Y-iPSC, and A-iPSC-GLUT3. Error bars indicate SEM of five biological replicates with three independent clones in each sample group. Statistical significance was determined by two-sided t test.

(B) MS-mediated histone modification profiling. A total of 99 different histone modifications was profiled by the MSKCC proteomics core. Statistically significantly different histone modifications between A-iPSC and Y-iPSC are presented. The exact number of biological replicates is indicated below each group. Statistical significance was determined by unpaired two-sided t test.